



Peripheral tissular analysis of rapamycin's effect as a neuroprotective agent in vivo

Alfredo Gonzalez-Alcocer¹ · Yareth Gopar-Cuevas¹ · Adolfo Soto-Dominguez¹ · Maria de Jesus Loera- Arias¹ · Odila Saucedo-Cardenas¹ · Roberto Montes de Oca-Luna¹ · Humberto Rodriguez-Rocha¹ · Aracely Garcia-Garcia¹

Received: 3 March 2022 / Accepted: 15 July 2022

© The Author(s), under exclusive licence to Springer-Verlag GmbH Germany, part of Springer Nature 2022

Abstract

Rapamycin is the best-characterized autophagy inducer, which is related to its antiaging and neuroprotective effects. Although rapamycin is an FDA-approved drug for human use in organ transplantation and cancer therapy, its administration as an antiaging and neuroprotective agent is still controversial because of its immunosuppressive and reported side effects. Therefore, it is critical to determine whether the dose that exerts a neuroprotective effect, 35 times lower than that used as an immunosuppressant agent, harms peripheral organs. We validated the rapamycin neuroprotective dosage in a Parkinson's disease (PD) model induced with paraquat. C57BL/6 J mice were treated with intraperitoneal (IP) rapamycin (1 mg/kg) three times per week, followed by paraquat (10 mg/kg) twice per week for 6 weeks, along with rapamycin on alternate days. Rapamycin significantly decreased dopaminergic neuronal loss induced by paraquat. Since rapamycin's neuroprotective effect in a PD model was observed at 7 weeks of treatment; we evaluated its effect on the liver, kidney, pancreas, and spleen. In addition, we prolonged treatment with rapamycin for 14 weeks. Tissue sections were subjected to histochemical, immunodetection, and morphometric analysis. Chronic rapamycin administration does not affect bodyweight, survival, and liver or kidney morphology. Although the pancreas tissular architecture and cellular distribution in Langerhans islets are modified, they may be reversible. The spleen B lymphocyte and macrophage populations were decreased. Notably, the lymphocyte T population was not affected. Therefore, chronic administration of a rapamycin neuroprotective dose does not produce significant tissular alterations. Our findings support the therapeutic potential of rapamycin as a neuroprotective agent.

Keywords Rapamycin · Chronic exposure · Histology · Neuroprotective dose · mTOR

Introduction

Rapamycin, a lipophilic macrolide antibiotic, is the best-characterized autophagy inducer, participating in cell growth, proliferation, and protein synthesis (Jung et al. 2010; Noda and Ohsumi 1998). Rapamycin is associated with beneficial effects on cancer (Anisimov et al. 2010, 2011; Heuer et al. 2012; Wang et al. 2013), diabetes (Xie and Herbert 2012; Long et al. 2012), tuberous sclerosis (Rosado et al. 2013; Wataya-Kaneda et al. 2012), cardiovascular diseases

(Selman and Partridge 2012; Comas et al. 2012; Chong and Maiese 2012; Ru et al. 2012), and neurological disorders (Tsang et al. 2007; Chong et al. 2010).

Rapamycin inhibits the serine/threonine kinase mammalian target of rapamycin (mTOR), and forms two protein complexes. The sensitivity of the mTOR complex 1 (mTORC1) and 2 (mTORC2) to rapamycin varies by cell line, tissue type, and exposure time. mTORC1 is a sensor for nutrient levels (amino acids and glucose) and insulin (Johnson et al. 2013a; Li et al. 2016; Vander Haar et al. 2007), while mTORC2 function is mediated by insulin/insulin-like growth factor 1 (IGF-1) signaling (Guertin et al. 2006; García-Martínez and Alessi 2008; Ikenoue et al. 2008; Liu et al. 2014). Interestingly, rapamycin is an acute and chronic inhibitor of mTORC1 and mTORC2, respectively.

Importantly, rapamycin immunomodulatory properties are widely used to prevent graft rejection after organ transplantation by inhibiting T and B cell proliferation (Khanna

✉ Aracely Garcia-Garcia
aracely.garciagr@uanl.edu.mx

Humberto Rodriguez-Rocha
humberto.rodriguezrc@uanl.edu.mx

¹ Departamento de Histología, Facultad de Medicina, Universidad Autónoma de Nuevo León, Francisco I. Madero S/N, 64460 Monterrey, Nuevo León, México

2000; Wicker et al. 1990; Mohacsi and Morris 1992; Lebowohl et al. 2013). However, its antiaging and prophylactic usage for neurodegeneration is still debated (Lamming et al. 2013; Lamming 2016) because of diverse side effects, including dyslipidemia, glucose intolerance, insulin resistance, new-onset diabetes, and gastrointestinal disorders (Johnston et al. 2008; McCormack et al. 2011; Gyurus et al. 2011; Lamming et al. 2012; Houde et al. 2010).

Rapamycin neuroprotective properties (Jiang et al. 2013; Malagelada et al. 2010; Ramirez-Moreno et al. 2019) are related to the autophagy induction (Chong et al. 2012; Graziotto et al. 2012; Mendelsohn and Larrick 2011) and have been achieved with a rapamycin dose 35 times lower than that used for immunosuppressive therapy (Jeon et al. 2018; Dominguez et al. 2000; Kahan et al. 1998; Saunders et al. 2001). Thus, we performed a peripheral tissular analysis to determine whether rapamycin neuroprotective dosage affects the liver, kidney, pancreas, and spleen to reassure its safety as an antiaging and prophylactic agent against neurodegeneration.

Materials and methods

Parkinson's disease animal model

C57BL/6J 8-week-old male mice (Circulo ADN, Mexico City) were randomly divided into four groups of six subjects each: (1) control, (2) rapamycin, (3) paraquat, and (4) rapamycin/paraquat. Mice were subjected to intraperitoneal (IP) injections of rapamycin (rapa) 1 mg/kg or PBS 1 × (control, ctrl) three times per week. After 1 week, it was followed by 10 mg/kg paraquat twice per week for six consecutive weeks and continued along with rapamycin treatment on alternate days. Mice were maintained on a 12-h light–dark cycle, with free access to Prolab RMH 2500 pellets (#5P14, LabDiet, St. Louis, MO) and drinking water.

Next, mice were anesthetized with an intramuscular injection of 10 mg/kg xylazine (#Q7833099, PiSA Labs, General Escobedo, Mexico) and 100 mg/kg ketamine (#Q7833028, PiSA Labs), followed by an IP injection of sodium pentobarbital (88 mg/kg). Afterward, mice were perfused intracardially with 4% paraformaldehyde (PFA) in 0.1 M sodium phosphate buffer (pH 7.4), and the brain was collected and post-fixed for 24 h in 4% PFA.

Chronic rapamycin neuroprotective dose administration

Mice were subjected to intraperitoneal (IP) injections of rapamycin (rapa) 1 mg/kg or PBS 1 × (control, ctrl) three times per week for 7 and 14 consecutive weeks. Mice bodyweight and survival were recorded weekly. The liver, kidney, pancreas, and spleen were collected and post-fixed for 24 h in 4% PFA.

Histological analysis

Fixed organs were processed in an Automated Tissue Processor (KD-TS3B, Zhejiang Jinhua Kedee Instrumental Equipment, Zhejiang, China) and embedded in paraffin blocks using a Tissue Embedding Center and Cooling System (KD-BM, Zhejiang Jinhua Kedee Instrumental Equipment). Sections of 5 μm were obtained using a sliding microtome (Model RM2235, Leica Biosystems, Wetzlar, Germany), stained with hematoxylin and eosin (H&E) or Mallory-Azan's Trichromic (collagen fibers), and examined in a Nikon light microscope (Eclipse 50i, Nikon, Melville, NY).

Bright-field images (×40) were acquired using the QCapture Pro 7™ software (QImaging Corporation, Surrey, BC, Canada). Morphometric analyses were performed using ImageJ (NIH) v3.91 software (<http://rsb.info.nih.gov/ij>). Liver images were used to count bi-nucleated hepatocyte number. The length of the renal corpuscle was measured in kidney images. In the pancreas, the Langerhans islet number with vascular dilation was determined. Finally, the spleen white pulp relative density was evaluated similarly to the method described by Syrjinen (1980).

Immunofluorescence

Midbrains were cut into 5-μm coronal sections, which were blocked with 10% normal horse serum (#16,050–122, Thermo Fisher Scientific) and incubated with rabbit anti-TH antibody (#ab112, Abcam) overnight at 4 °C. After rinsing, sections were incubated with secondary Alexa 488 anti-rabbit (#ab150077, Abcam) for 1 h at room temperature (RT).

Pancreas sections were incubated with primary rabbit anti-insulin antibody (#ab181547, Abcam, Cambridge, UK) or rabbit anti-glucagon (#ab92517, Abcam) overnight at 4 °C. Next, sections were incubated with secondary Alexa 594 anti-rabbit (#ab150080, Abcam) for 1 h at RT. All antibodies were diluted 1:1000.

Sections were mounted with VECTASHIELD Antifade Mounting Medium with DAPI. Images were collected on a Nikon® Eclipse 50i fluorescent microscope and analyzed using ImageJ software. From midbrain sections, tyrosine hydroxylase (TH) fluorescence intensity was quantified.

In pancreas sections, islet number with cell disorganization was determined. Insulin and glucagon fluorescence intensity was evaluated in four random fields per section. Corrected total cell fluorescence (CTCF) was obtained with the following formula:

$$\text{CTCF} = \text{Integrated Density} - (\text{Area of selected cell} \times \text{Mean fluorescence of background readings}).$$

Immunohistochemistry

Pancreas sections were subjected to IHC using primary rabbit anti-insulin overnight at 4 °C. Spleen sections were

subjected to IHC using the following antibodies: rabbit anti-CD3 (#A0452, Dako, EUA), rabbit anti-CD4 (#sc-1140, Santa Cruz Biotechnology, Dallas, TX), rabbit anti-CD8 (#sc-7188, Santa Cruz Biotechnology), mouse anti-CD20 (#sc-7735, Santa Cruz Biotechnology), and rabbit anti-CD68 (#ab22506, Abcam) diluted 1:500; secondary rabbit (#sc-2257, Santa Cruz Biotechnology) and mouse (#ab6789, Abcam) antibodies were diluted 1:1000.

By using the “polygon” tool, the positive area (mm²) for every specific antibody signal (T lymphocytes CD3⁺, cytotoxic lymphocytes CD8⁺, helper lymphocytes CD4⁺, B lymphocytes CD20⁺, and macrophages CD68⁺) was delimited in ten random fields ($\times 10$) per subject, in a total of three subjects per group.

Statistical analysis

All experiments were performed independently on separate days. The Shapiro–Wilk test determined that our data were normally distributed. Next, TH fluorescence intensity data were analyzed by one-way ANOVA with a Šidák's multiple comparisons test. Bodyweight, bi-nucleated hepatocyte number, renal corpuscles' size, islet number with vascular dilation, white pulp density, and all immunodetection morphometries were analyzed by two-way ANOVA with Tukey's multiple comparison test. The survival was assessed with a Log-rank (Mantel-Cox) test. The number of islets with alpha-cell disorganization and glucagon fluorescence intensity was evaluated with a paired *t*-test, while LC3-II, phosphorylated (pS2448) mTOR WB's, and insulin expression were evaluated with an unpaired *t*-test. Data were plotted as mean values of at least three independent replicas \pm SEM. A *p*-value of *p* < 0.05 was considered statistically significant for all the analyses. Our *p*-values' summary is as follows: ns > 0.05, * < 0.05, ** < 0.001, **** < 0.0001. Statistical software Prism 6 (GraphPad Software, San Diego, CA) was used.

Results

Rapamycin decreases dopaminergic neuronal loss in a Parkinson's disease model

We (Ramirez-Moreno et al. 2019) and others (Jiang et al. 2013; Malagelada et al. 2010) have previously demonstrated the rapamycin neuroprotective effect in a Parkinson's disease model. First, we validated this effect where midbrain dopaminergic neurons were examined. Figure 1a shows the typical dopaminergic neuronal population from the control group, which was not affected by rapamycin treatment. Parkinson's disease model was induced with the herbicide paraquat, which induced a noticeable decrease

in dopaminergic neurons compared to the control group. Importantly, rapamycin treatment decreased dopaminergic neuronal loss induced by paraquat. These results were corroborated by quantifying tyrosine hydroxylase (TH) fluorescence intensity (Fig. 1b).

Chronic rapamycin exposure does not affect bodyweight and survival

Because of rapamycin immunosuppressant properties, it is essential to determine whether chronic exposure to this agent causes morphological changes in vivo. Mice were randomly divided into two groups that received PBS 1 \times (control) or rapamycin. Mice bodyweight (Fig. 2a) and survival (Fig. 2b) were recorded throughout 14 weeks of treatment. Both groups present a normal distribution without statistical difference. Therefore, chronic exposure to 1 mg/kg rapamycin does not affect mice's bodyweight and survival.

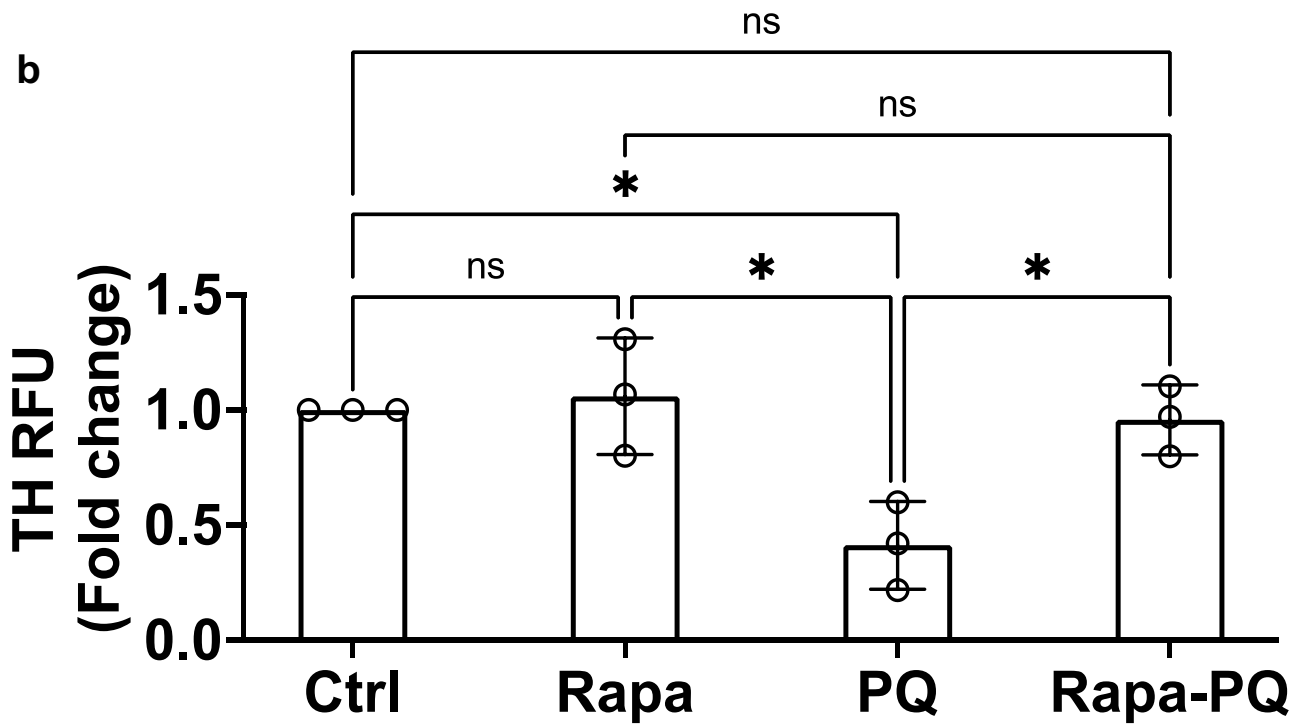
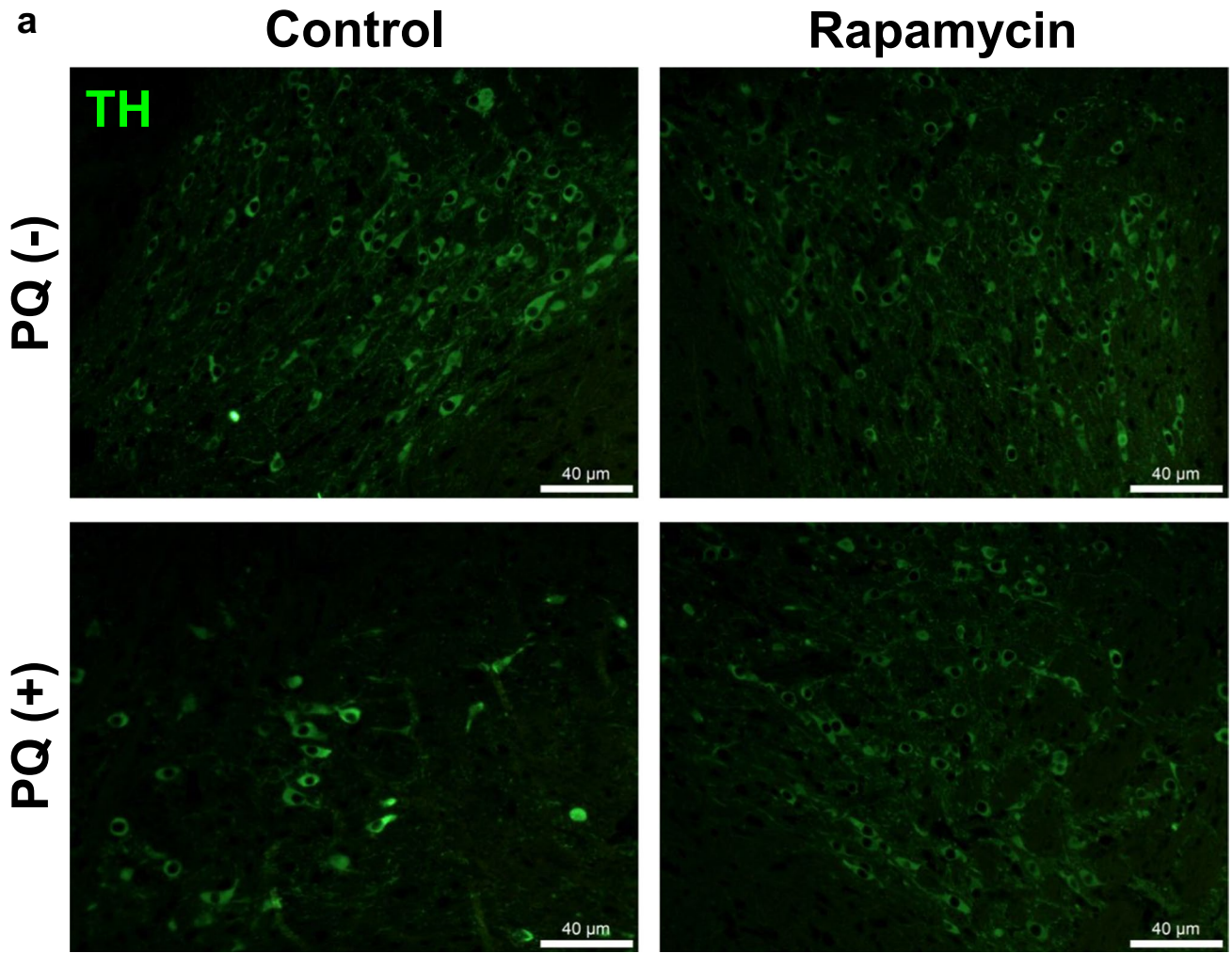
Chronic treatment with rapamycin induces an increase of the autophagy hallmark LC3-II in the pancreas

One of the most striking properties of rapamycin is its neuroprotective effect (Li 2009) mediated by autophagy, which has been achieved even with a dose 35 times lower (Ramirez-Moreno et al. 2019; Jeon et al. 2018; Dominguez et al. 2000; Kahan et al. 1998; Saunders et al. 2001) than that used for immunosuppressive purposes. Autophagy mediated by rapamycin depends on the mammalian target of rapamycin (mTOR) inhibition by direct binding to mTORC1, a nutrient-sensitive kinase (Schriever et al. 2013; Poüs and Codogno 2011), and by blocking mTOR phosphorylation (Malagelada et al. 2010; Sarkar et al. 2008).

The autophagy marker LC3-II and mTOR phosphorylation were evaluated in the liver (Supplementary Fig. 1a) and pancreas (Supplementary Fig. 1b) protein extracts by Western blot. LC3-II was increased in the pancreas but not in the liver. Meanwhile, mTOR phosphorylation decreased with no statistically significant difference in both organs in response to rapamycin compared to the control.

Liver morphology is not affected by chronic administration of rapamycin

Since detoxification of harmful compounds occurs in the liver, we wanted to determine whether rapamycin affects its morphology. Normal morphology consisting of sinusoids traveling and draining toward the central vein surrounded by hepatocytes strips (Fig. 3a and Supplementary Fig. 2), and the scarce presence of collagen fibers (Fig. 3b), were observed at 7 and 14 weeks in both the control and rapamycin-treated groups. Accordingly, the number of bi-nucleated



◀**Fig. 1** Dopaminergic neuronal death induced by paraquat is decreased by rapamycin. **a** Midbrain sections were subjected to IF with anti-TH to detect dopaminergic neurons, which were decreased in response to paraquat, while this effect was prevented by rapamycin. **b** TH fluorescence intensity was quantified in four random fields per section. Data were analyzed by one-way ANOVA with a Šídák's multiple comparisons test and plotted as mean values of at least three independent replicas \pm SEM. A *p*-value of $*p < 0.05$ was considered statistically significant. Rapa, rapamycin; PQ, paraquat

hepatocytes was analyzed (Fig. 3c), and there was no change after 14 weeks. Therefore, rapamycin did not cause any histological alteration in mice livers.

Chronic exposure to rapamycin does not affect kidney morphology

Because most drugs are excreted through the kidneys, we asked whether rapamycin alters their tissular architecture. Kidneys' regular organization was observed in the control and rapamycin-treated mice at the indicated times. Representative micrographs are shown in Fig. 4a and Supplementary Fig. 3, displaying a renal corpuscle with a central glomerulus; the Bowman's space between its visceral and parietal layers; transverse segments of proximal and distal convoluted tubules; and short collagen fibers (Fig. 4b). Renal corpuscles' size was analyzed (Fig. 4c), and no changes were observed in both groups. These results indicate that rapamycin did not cause histological alterations in mice kidneys.

Pancreas tissular architecture and cell distribution are modified in response to chronic rapamycin administration

mTOR also plays a role in the pancreatic Langerhans islet development, beta-cell growth, and insulin processing and secretion (Bartolome and Guillén 2014; Blandino-Rosano et al. 2017; Elghazi et al. 2017; Li et al. 2016; Sinagoga et al. 2017). Thence, we aimed to investigate whether the rapamycin dose we used impacts the pancreas histological arrangement. Figure 5a and Supplementary Fig. 4 show the typical pancreatic acini and Langerhans islets in the control group. The exocrine pancreas of the rapamycin-treated group did not show histological alterations. However, dilated capillaries were detected in the Langerhans islet at 7 weeks of treatment with rapamycin (Fig. 5c) and were similar to those of the control group at 14 weeks. Figure 5b displays the longitudinal arrangement of collagen fibers forming the pancreatic septum in the control group. Nevertheless, septum fibers were distributed within the exocrine and endocrine pancreas in the rapamycin-treated groups.

Moreover, it has been reported that rapamycin treatment can lead to glucose intolerance development in rodents and humans (Houde et al. 2010; Teutonico et al. 2005;

Cunningham et al. 2007). Then, we sought to investigate whether chronic rapamycin exposure could alter Langerhans islets' cellular organization. We used specific antibodies recognizing insulin and glucagon produced by the beta- and alpha-cells, respectively. When detected by IHC, the insulin signal was increased in response to rapamycin compared to the control (Supplementary Fig. 5). In contrast, IF showed no differences in the beta-cell population (Fig. 6a).

Interestingly, compared to the control group, where alpha-cells exhibit the typical distribution in the Langerhans islet periphery, in response to rapamycin, the alpha-cells pattern was disrupted at both treatment times, arranged throughout the islet (Fig. 6b). The number of islets with alpha-cell disorganization (Fig. 6c) and glucagon fluorescence intensity (Fig. 6d) analysis show statistical differences between groups. These results showed that chronic rapamycin administration induces capillaries dilation, modifies the collagen distribution, and alters alpha-cell organization.

Spleen lymphocytes B and macrophages population are altered in response to chronic rapamycin administration

Due to rapamycin immunosuppressant properties inhibiting T and B cell proliferation (Khanna 2000; Wicker et al. 1990; Mohacsi and Morris 1992), we evaluated whether a dose of rapamycin 35 times lower than that used for organ transplantation affects the spleen, a lymphatic organ. Figure 7a shows the typical spleen organization in the control group, where the white (lymph nodes) and red pulp are included and are also preserved in the rapamycin-treated groups at the analyzed times. Collagen fibers in blue also show a typical organization and are particularly abundant surrounding arteries (Fig. 7b). Withe pulp density was analyzed, and no differences were observed between groups (Fig. 7c).

We used specific antibodies recognizing the different lymphoid lineages to evaluate the possible rapamycin's inhibiting effect on T and B cell proliferation. Figure 8 shows IHC detecting (a) T lymphocytes, (c) helper T lymphocytes, (e) cytotoxic T lymphocytes, (g) B lymphocytes, and (i) macrophages. The corresponding morphometric analyses are shown on the right (Fig. 8b, d, f, h, j), finding a statistically significant decrease in B lymphocytes and macrophages populations at 14 weeks of treatment with rapamycin. Therefore, chronic rapamycin administration in vivo does not cause morphological changes in the spleen or alter the lymphocyte T population. Conversely, rapamycin affects lymphocytes B and macrophages population.

Discussion

Although rapamycin is an FDA-approved drug for human use in organ transplantation and cancer therapy, its administration as an antiaging and neuroprotective agent is still

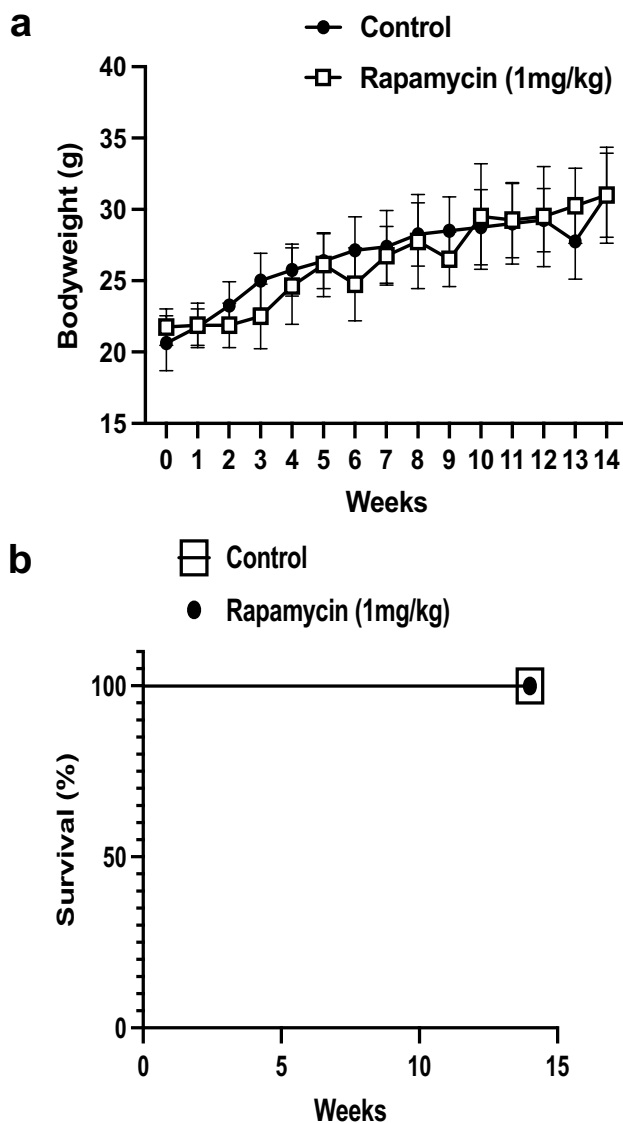


Fig. 2 Chronic administration of rapamycin in vivo does not alter body weight or survival. During 7 and 14 weeks, mice were exposed to rapamycin three times per week, and PBS 1× was administered to the control group. **a** Bodyweight and **b** survival were recorded throughout 14 weeks of treatment. Both groups present a normal distribution without statistical difference. $n=6$ animals per group. Bodyweight were analyzed by two-way ANOVA with a Tukey's multiple comparisons test whereas survival was assessed with a Log-rank (Mantel-Cox) test. Data were plotted as mean values of at least three independent replicas \pm SEM. A p -value of $*p < 0.05$ was considered statistically significant. Bodyweight and survival p -value ns > 0.05

controversial because of its immunosuppressive side effects. However, rapamycin, wrongly stereotyped as an “immunosuppressor,” is, in fact, an immunomodulator (Bravo-San Pedro and Senovilla 2013; Mannick et al. 2014, 2018; Blagosklonny 2019).

As mentioned before, rapamycin is a negative regulator of mTOR; the latter is activated by nutrients and insulin

leading to insulin signaling inhibition and producing insulin resistance (Krebs et al. 2007; Tremblay et al. 2005). Therefore, rapamycin emulates starvation conditions (Longo and Fontana 2011). Acute (Krebs et al. 2007; Leontieva et al. 2014) and chronic (Deblon et al. 2012) rapamycin treatment prevented insulin resistance.

Various long-term metabolic effects of rapamycin are reported in humans (Johnston et al. 2008; McCormack et al. 2011; Gyurus et al. 2011; Lamming et al. 2012; Houde et al. 2010). Notably, most of the side effects evidence comes from relatively ill subjects and studies lacking a placebo group, and healthy subjects may experience fewer serious side effects.

Short-term rapamycin treatment is currently used in organ transplantation and cancer therapy. Organ transplant recipients are subjected to immunosuppressive therapy to avoid rejection, which is associated with an increased death incidence from malignancies (Kauffman et al. 2005). However, rapamycin prevents cancer in organ transplantation patients (Mathew et al. 2004; Kauffman et al. 2005; Campistol et al. 2006; Lebranchu 2010).

Although there is evidence supporting rapamycin's antiaging and neuroprotective effects (Jiang et al. 2013; Malagelada et al. 2010; Ramirez-Moreno et al. 2019), its use is not approved for age-related conditions. Most likely, short-term rapamycin treatment is insufficient for age-related diseases. Importantly, rapamycin's antiaging properties, including its neuroprotective function, demand a long-term treatment to exert the best results; thus, it is critical to demonstrate that rapamycin does not have life-threatening effects. Indeed, many of the rapamycin's adverse side effects could be mitigated through intermittent dosing or rapamycin analogs (Arriola Apelo et al. 2016).

Oral (Barriocanal-Casado et al. 2019; Johnson et al. 2015; Felici et al. 2017; Siegmund et al. 2017) and intraperitoneal (IP) (Johnson et al. 2013b; Khan et al. 2017; Civiletto et al. 2018) rapamycin administration results in a life expectancy improvement. However, there are differences depending on the time and dosage used.

Using an allometric scaling, we can extrapolate the neuroprotective dose of rapamycin used in our model to that used in humans based on the dose normalization to the body surface area and considering the treatment scheme (Nair and Jacob 2016; Volunteers 2002). This approach assumes some unique characteristics of anatomical, physiological, and biochemical processes among species and the possible difference in pharmacokinetics/physiological time. This method is frequently used in research to predict an approximate dose based on data existing in other species (Nair and Jacob 2016; Volunteers 2002). So, the neuroprotective dose of rapamycin (1 mg/kg) used in our model is 35× lower than the maximum dose of rapamycin used in humans with low-to-moderate immunologic risk.

Fig. 3 Chronic administration of rapamycin *in vivo* does not induce morphological changes in the liver. **a** H&E staining shows a central vein (red star) surrounded by hepatocytes strips (red lines); between these strips, sinusoids are traveling and draining toward the central vein. No histological alteration was observed in rapamycin-treated mice at the indicated times. **b** Mallory-Azan trichrome staining. The scarce presence of collagen fibers, which appear in blue, is observed in the control and rapamycin-treated groups. **c** Statistical analysis of the number of bi-nucleated hepatocytes from 3 independent experiments. Data were analyzed by two-way ANOVA with a Tukey's multiple comparisons test and plotted as mean values of at least three independent replicas \pm SEM. A *p*-value of $*p < 0.05$ was considered statistically significant

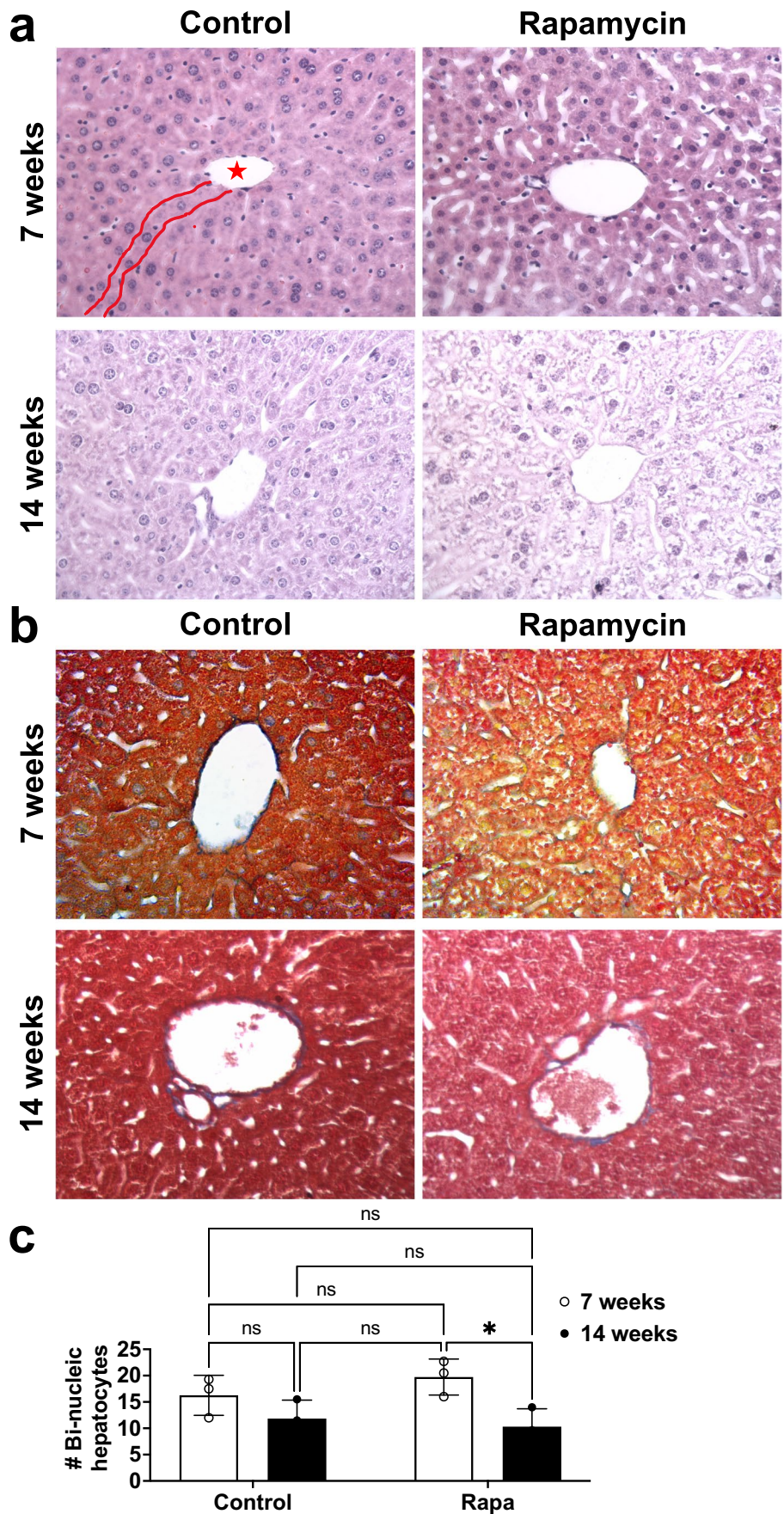


Fig. 4 Chronic administration of rapamycin *in vivo* does not affect kidney morphology. **a** H&E staining displaying a renal corpuscle with a central glomerulus (red star), with its visceral layer (blue line), between the latter and the parietal layer (red line) lays out the Bowman's space. Transverse segments of proximal (red arrowhead) and distal convoluted tubules (red arrow) are also seen in the micrograph. No morphological changes were observed in rapamycin-treated mice at the indicated times. **b** Mallory-Azan trichrome staining shows the scarce presence of collagen fibers in the control and rapamycin-treated groups, all with normal histology. **c** Statistical analysis of the renal corpuscles' size from 3 independent experiments. Data were analyzed by two-way ANOVA with a Tukey's multiple comparisons test and plotted as mean values of at least three independent replicas \pm SEM. A *p*-value of $*p < 0.05$ was considered statistically significant. Renal corpuscles' size *p*-value $ns > 0.05$

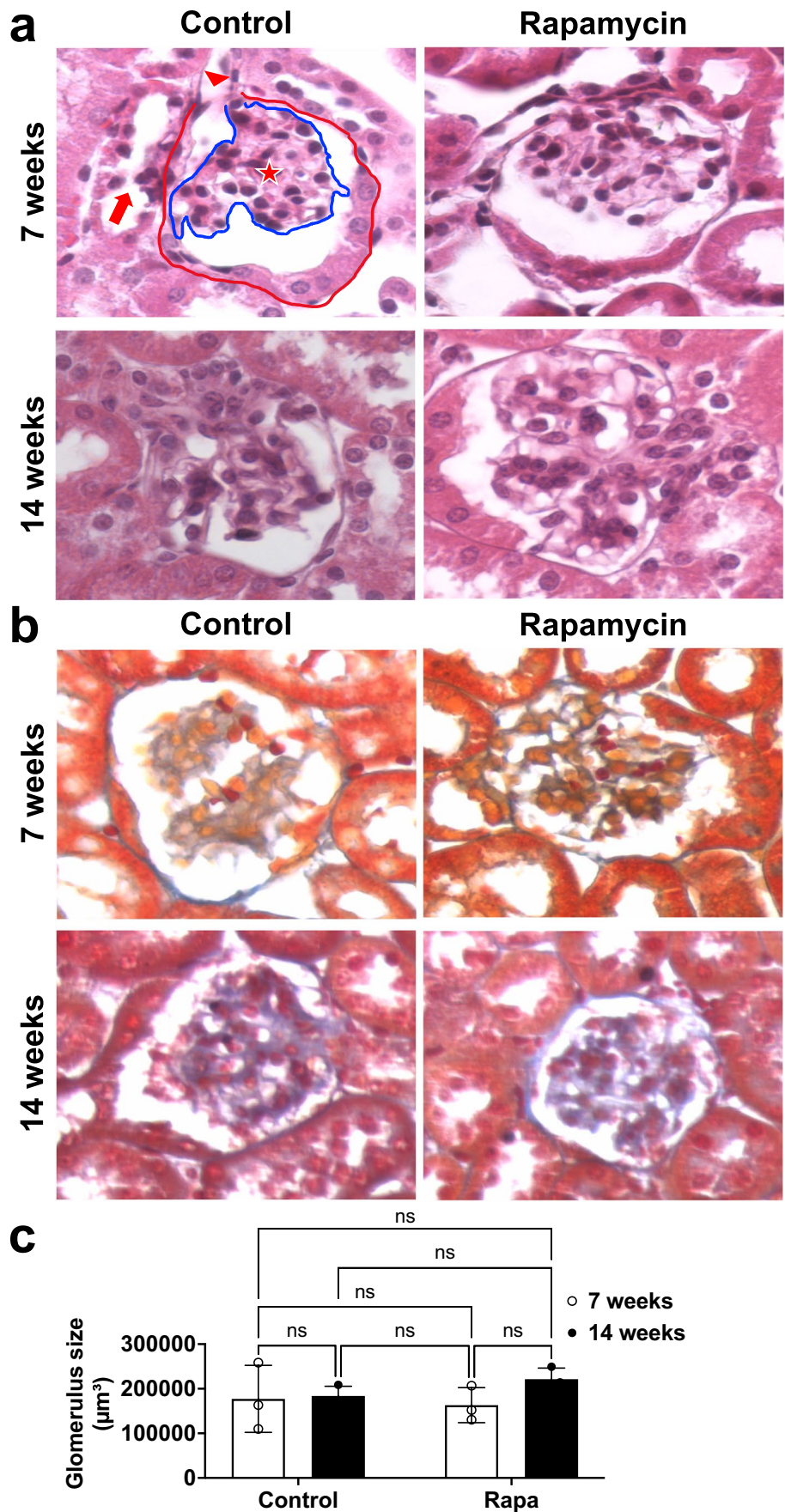


Fig. 5 Chronic administration of rapamycin *in vivo* causes morphological changes in the pancreas. **a** H&E staining shows the typical histological organization of the pancreatic acini (exocrine, blue line) and islets of Langerhans (endocrine, red line) in the control group. The exocrine pancreas of the rapamycin-treated group does not show any histological alteration, while the Langerhans islets' capillaries are dilated (red star) after 7 weeks of treatment; and after 14 weeks are similar to that of the control. **b** Mallory-Azan trichrome staining shows the longitudinal arrangement of collagen fibers, forming the control group's pancreatic septum (red arrow). The septum fibers are distributed within the exocrine and endocrine (red arrowhead) pancreas in the rapamycin-treated groups. **c** Statistical analysis of the number of islets with vascular dilation from 3 independent experiments. Data were analyzed by two-way ANOVA with a Tukey's multiple comparisons test and plotted as mean values of at least three independent replicas \pm SEM. A *p*-value of $*p < 0.05$ was considered statistically significant. Islets with vascular dilation *p*-value $ns > 0.05$

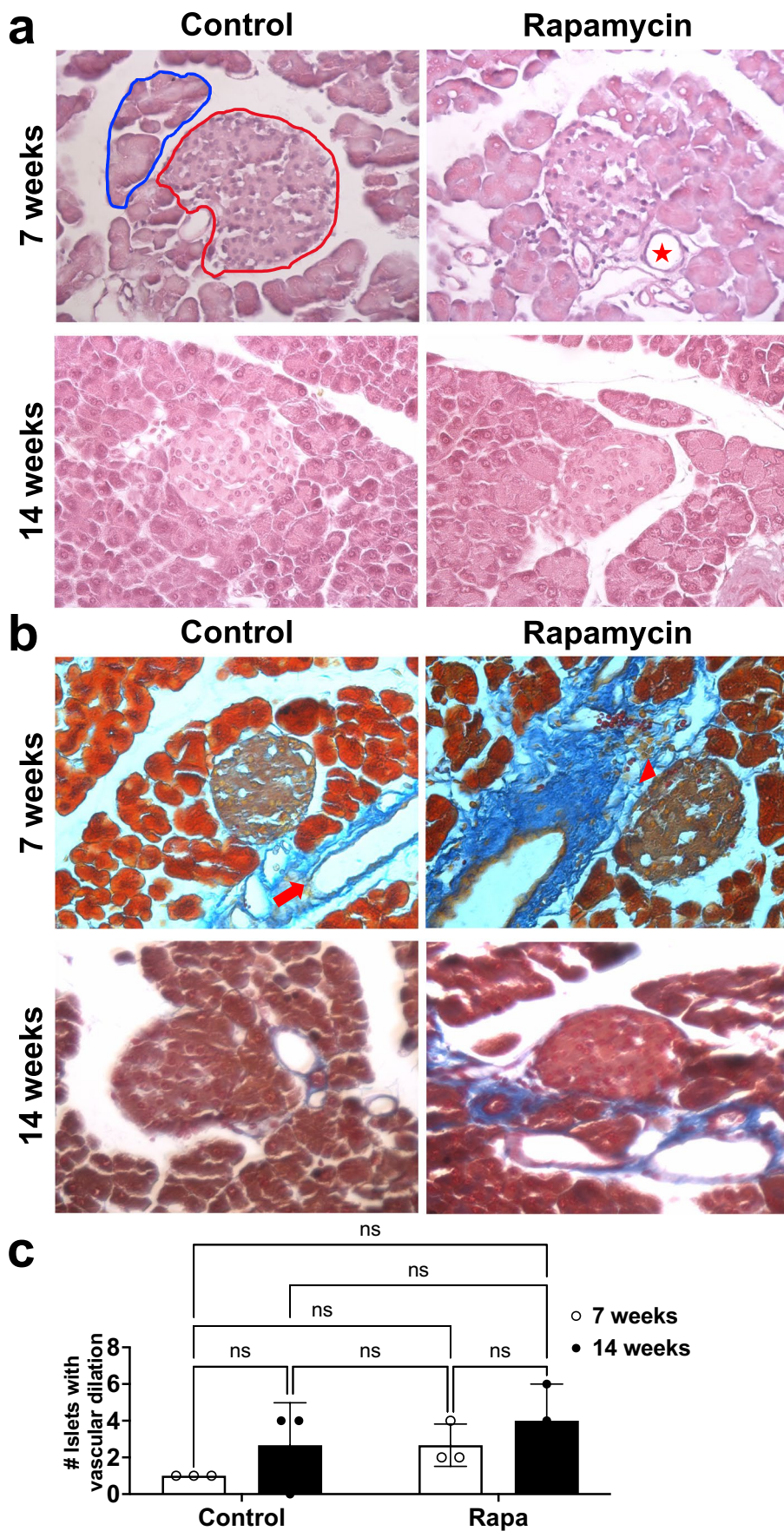


Fig. 6 Rapamycin alters the alpha-cell distribution of the islet of Langerhans. **a** IF was used to identify the beta-cell population with a specific anti-insulin antibody. Both control and rapamycin groups present a normal distribution of cells. **b** The alpha-cell population was identified with a specific anti-glucagon antibody. The control group exhibits the normal distribution of alpha-cells in the Langerhans islet periphery, while this pattern is disrupted in both rapamycin groups, where alpha-cells are arranged throughout the islet (blue arrowheads). **c** Statistical analysis of the number of islets with alpha-cell disorganization from 3 independent experiments at 7 weeks of treatment. **d** Statistical analysis of glucagon fluorescence intensity from 3 independent experiments at 7 weeks of treatment. Data were analyzed by paired *t* test and plotted as mean values of at least three independent replicas \pm SEM. A *p*-value of $*p < 0.05$ was considered statistically significant. Islets with alpha-cell disorganization $*p < 0.05$, while glucagon fluorescence intensity *p*-value $ns > 0.05$

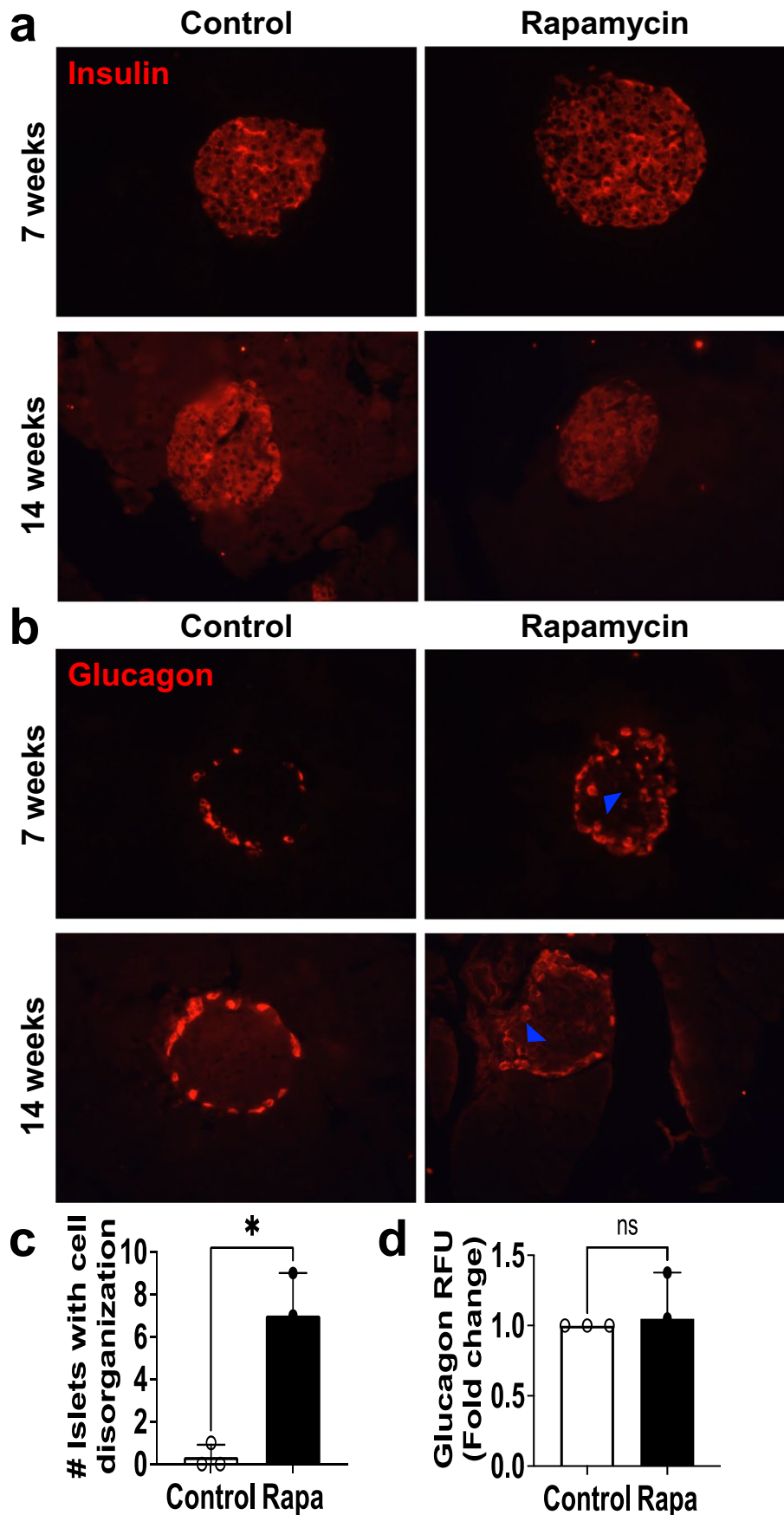


Fig. 7 Chronic administration of rapamycin *in vivo* does not cause morphological changes in the spleen. **a** H&E staining where the white pulp (red arrow), the red pulp (red arrowhead), and lymph nodes (red star) are observed, all with a typical organization in the control and rapamycin-treated groups at the analyzed times. **b** Mallory-Azan trichrome staining, where collagen fibers in blue show a typical organization and are particularly abundant surrounding arteries (black star). **c** Statistical analysis of the white pulp density from 3 independent experiments. Data were analyzed by two-way ANOVA with a Tukey's multiple comparisons test and plotted as mean values of at least three independent replicas \pm SEM. A *p*-value of $*p < 0.05$ was considered statistically significant. White pulp density *p*-value $ns > 0.05$

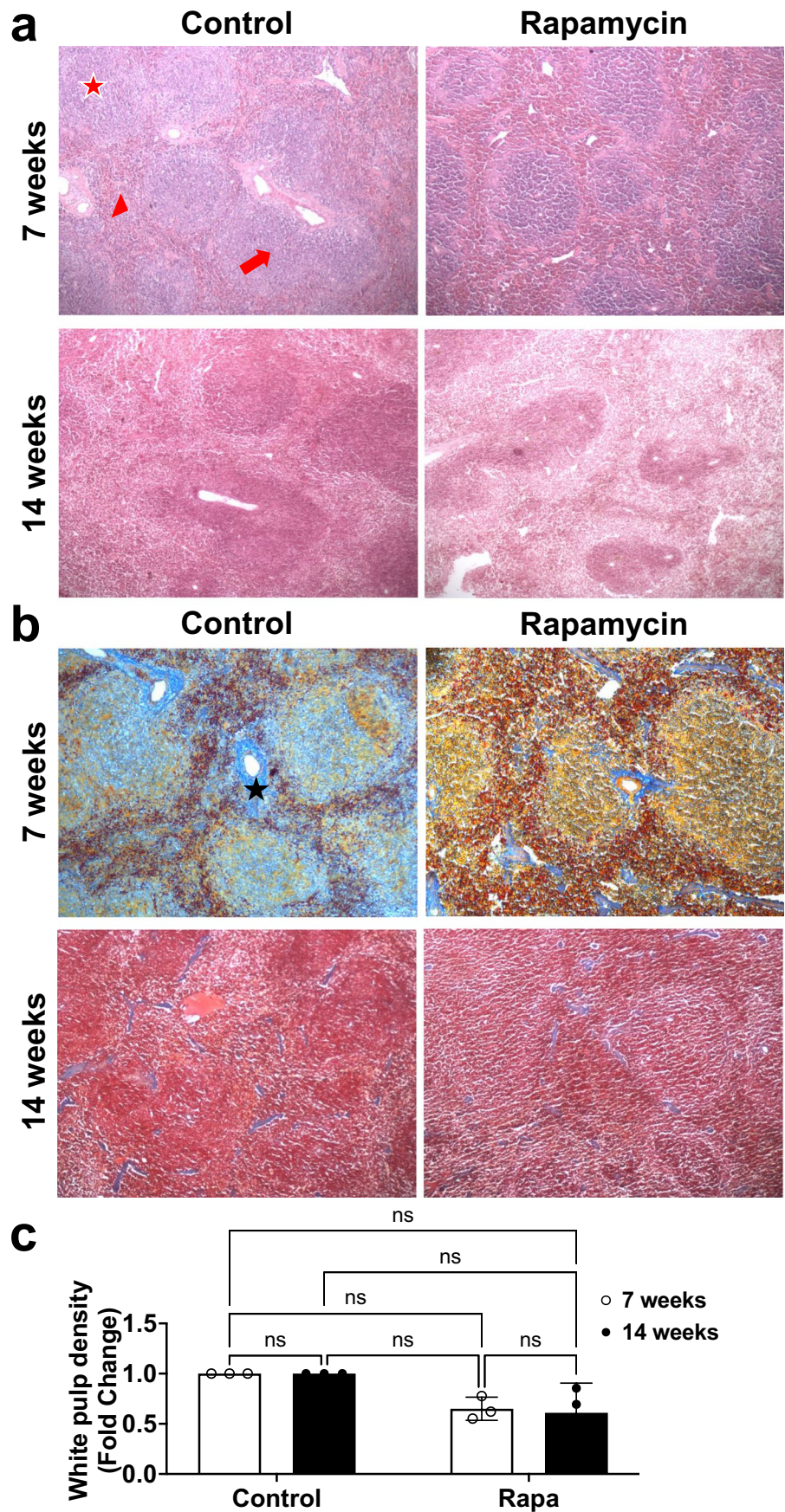
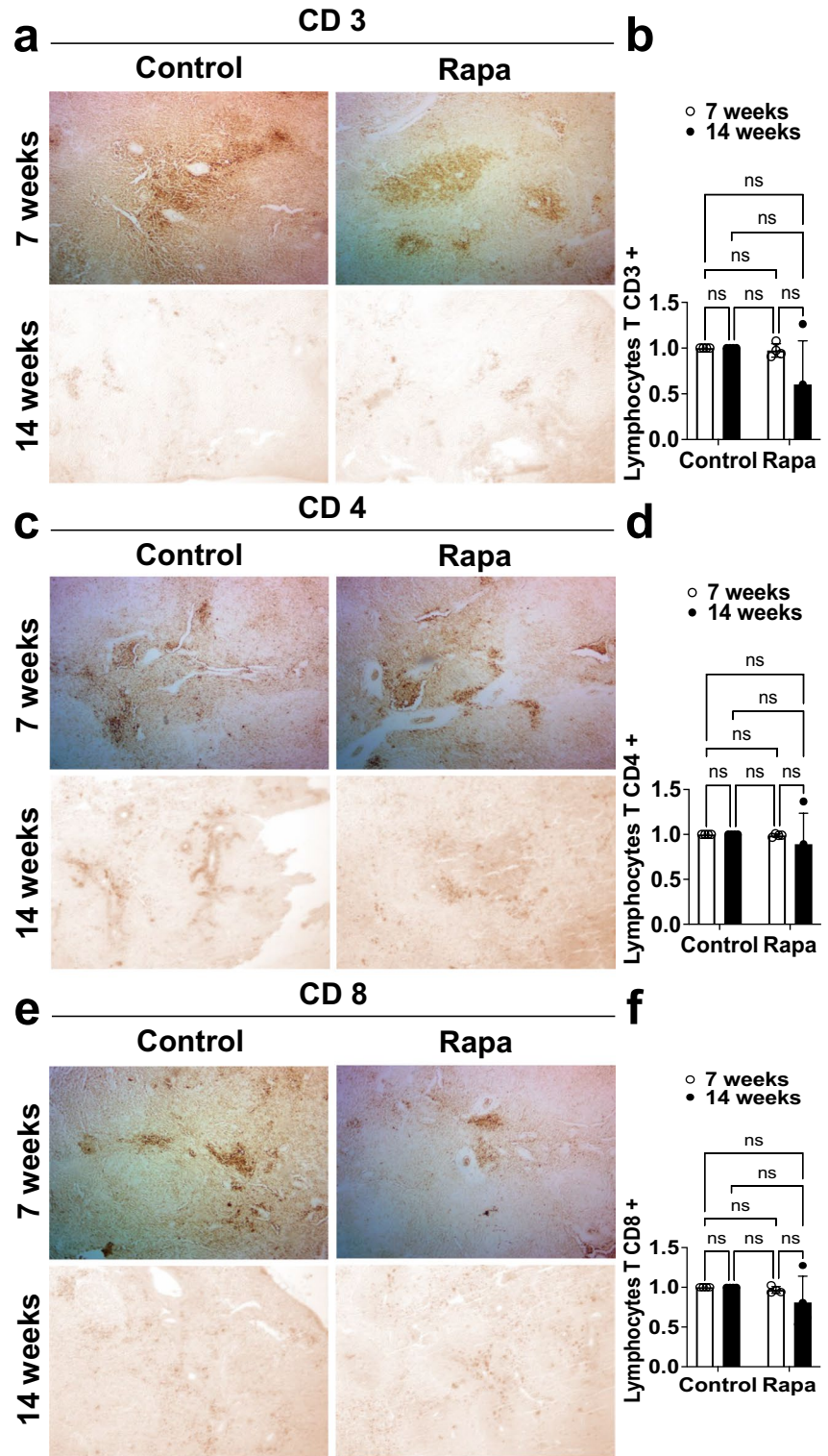


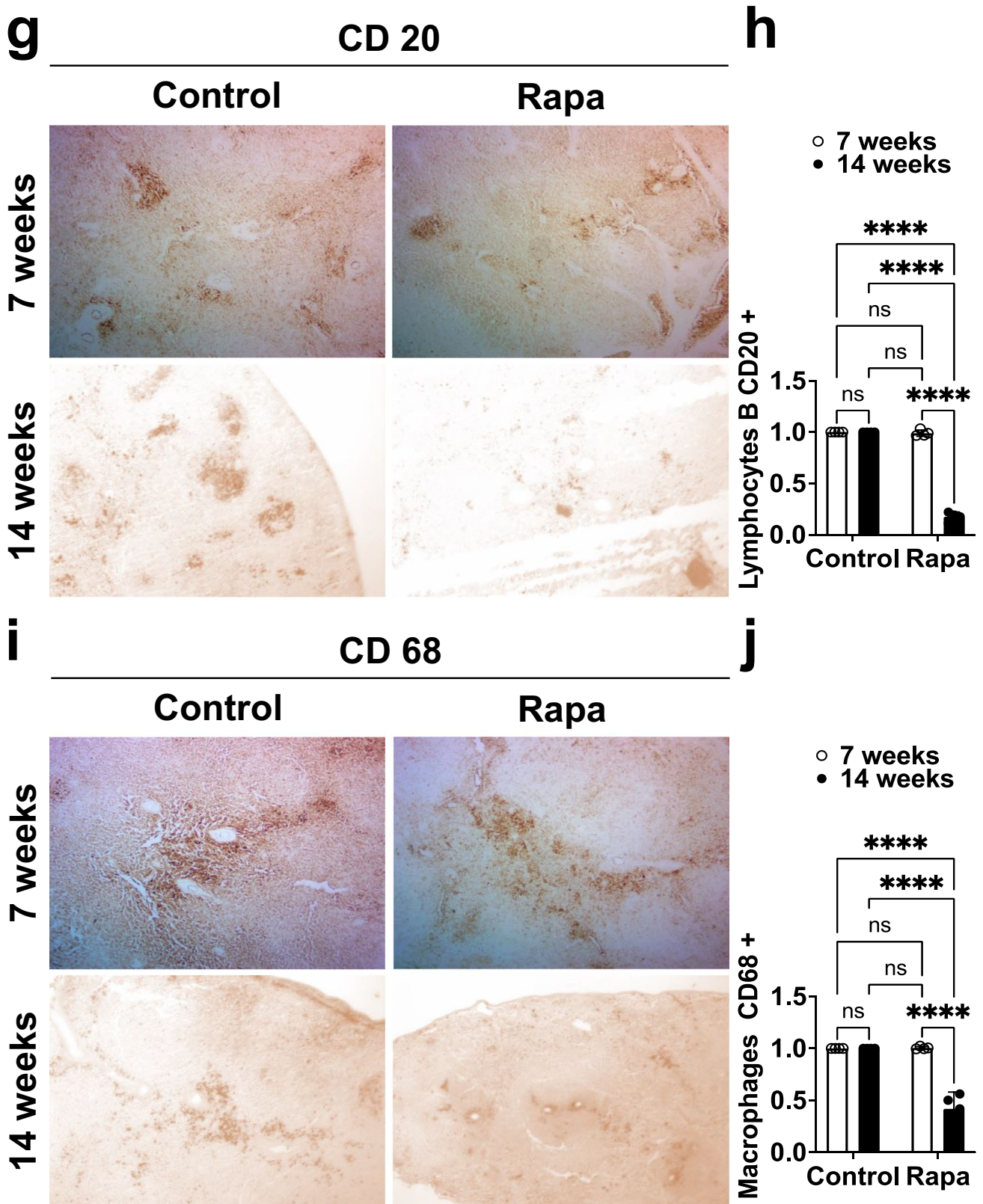
Fig. 8 Chronic administration of rapamycin in vivo does not alter the lymphocyte T population but lymphocytes B and macrophages. IHC detecting (a) T lymphocyte with a specific anti-CD3 antibody; (c) helper T lymphocyte, using a specific anti-CD4 antibody; (e) cytotoxic T lymphocyte, with a specific anti-CD8 antibody; (g) B lymphocytes using a specific anti-CD20 antibody; and (i) macrophages with a specific anti-CD68 antibody. **b, d, f, h, j** Morphometric analysis from 3 independent experiments of each immunodetection showed a statistical difference in B lymphocytes and macrophages after 14 weeks of treatment with rapamycin. Data were analyzed by two-way ANOVA with a Tukey's multiple comparisons test and plotted as mean values of at least three independent replicas \pm SEM. A p -value of $*p < 0.05$ was considered statistically significant. Lymphocyte T CD3+, lymphocyte T CD4+, and lymphocyte T CD8+ p -value ns > 0.05 , while lymphocyte B CD20+ and macrophage CD68+ $***p < 0.0001$



Therefore, we evaluated the effect of chronic exposure (14 weeks) of a neuroprotective dose of rapamycin, which is 35 times lower than that used as an immunosuppressive agent. We confirmed that our dosing schedule does not affect bodyweight or survival in an in vivo model.

Since the underlying neuroprotective mechanism of rapamycin is mediated by autophagy induction (Chong et al. 2012; Graziotto et al. 2012; Mendelsohn and Larrick 2011) by blocking mTOR complex phosphorylation (Malagelada et al. 2010; Sarkar et al. 2008), we showed that rapamycin

Fig. 8 (continued)



does indeed induce an increase in the autophagy hallmark, LC3-II, and the mTOR complex phosphorylation is decreased in the liver and pancreas, compared to the control group.

Detoxification of harmful compounds occurs in the liver, and most drugs are excreted through the kidneys. However, the rapamycin sensitivity varies by cell line and tissue type. For example, the liver was sensitive to the rapamycin effects, which did not occur in the kidney (Sarbasov et al. 2006; Schreiber et al. 2015). Despite the evident inhibition of mTORC1 by high rapamycin doses, no autophagy induction was observed in the brain, heart, liver, and kidney (Barriocanal-Casado et al. 2019). We evaluated the liver and kidney morphology, concluding that chronic rapamycin administration does not affect liver or kidney histology. Also, the rapamycin sensitivity to the mTOR complex is relevant for research as it may be the key to balancing the drug's benefits and adverse side effects.

The mTOR complex also plays a role in developing the pancreatic Langerhans islets, the beta-cell growth, and the insulin processing and secretion (Bartolome and Guillén 2014; Blandino-Rosano et al. 2017; Elghazi et al. 2017; Li et al. 2016; Sinagoga et al. 2017). Experimental rapamycin treatment causes glucose intolerance in rodents and humans (Houde et al. 2010; Teutonico et al. 2005; Cunningham et al. 2007). We observed that pancreatic histological architecture and cell distribution are modified in response to chronic rapamycin administration. Notably, it has been reported that although long-life treatment may conduce to developing a diabetes-like condition (Blagosklonny 2011), it is reversible and does not lead to complications (Blagosklonny 2019).

Finally, we analyzed the spleen, a lymphatic organ, because of rapamycin's immunomodulatory properties. We found that rapamycin neuroprotective dose affects the spleen by decreasing the B lymphocytes and macrophages population. Notably, the lymphocyte T population was not affected. A study in mice where daily or intermittent rapamycin treatment regimen consisted of treatment with 2 mg/kg rapamycin 1 ×/day or 1 ×/5 days for 8 weeks showed by flow cytometry that daily rapamycin treatment impacted CD3⁺CD4⁺ T cell and CD3⁺CD8⁺ T cell numbers more than the intermittent rapamycin treatment regimen (Arriola Apelo et al. 2016). The study above used twice the rapamycin concentration we used in our study, and our administration regimen was three times per week for 7 and 14 consecutive weeks, and we did not observe changes in CD3⁺CD4⁺ T cell and CD3⁺CD8⁺ T cells in situ by IHC. It is worth noticing that flow cytometry is a more sensitive method for cell counting, while IHC locates cells directly in tissue sections, and the morphometric analysis is semi-quantitative. However, our data were consistent in both rapamycin administration regimens. Although we observed no impact of rapamycin on the lymphocyte T population,

one of the limitations of our study is that we did not evaluate the immune effector cell function. Immune effector cell function was evaluated in mice daily treated with IP acute rapamycin (75 µg/kg) scheme, 2 days before being subjected to viral or intracellular bacterial infection and lasted for 7 days post-infection, where functional CD8 T cell and macrophage were depressed (Goldberg et al. 2014). It was shown that rapamycin enhances memory CD8 T cell differentiation at the cost of effector differentiation by blocking glycolytic metabolism. In addition, primary cultures of mice and human macrophages treated with rapamycin during bacterial infection showed a decreased lysosomal acidification, resulting in an impaired function (Goldberg et al. 2014). Even though we did not test the macrophage lysosomal acidification, we observed that the macrophages and B lymphocytes, both antigen-presenting cells, decreased in rapamycin-treated mice. Also, it is worth noticing that in our model, mice's bodyweight and survival were not compromised in response to rapamycin. However, more studies are required to determine whether the neuroprotective dose of rapamycin we used impacts the immune effector cell function.

In summary, our findings support the rapamycin's therapeutic potential as a neuroprotective agent as its chronic administration does not affect bodyweight or survival, neither liver nor kidney morphology. Although the pancreas histological architecture and Langerhans islets' cellular distribution are modified, they may be reversible. Also, the spleen B lymphocyte and macrophage populations were decreased, but lymphocyte T were not affected.

Supplementary Information The online version contains supplementary material available at <https://doi.org/10.1007/s00210-022-02276-6>.

Acknowledgements Graphical abstract was created with Biorender.com.

Author contribution AGA, YGC, and ASD performed the research; AGG and HRR designed the research study; AGA, MJLA, OSC, RMOL, HRR, and AGG analyzed the data; AGA, HRR, and AGG wrote the paper. All authors read and approved the manuscript. The authors declare that all data were generated in-house and that no paper mill was used.

Funding This work was supported by the National Council of Science and Technology (Consejo Nacional de Ciencia y Tecnología, CONACYT: CB-2013–221615) and Programa de Apoyo a la Investigación Científica y Tecnológica (PAICYT) SA097-15.

Data availability All data generated or analyzed during this study are included in this manuscript and its supplementary information files.

Declarations

Ethical approval All experiments were conducted following the Mexican Official Norm "NOM-062-ZOO- 1999" and the Institutional Com-

mittee for the Care and Use of Laboratory Animals CICUAL (Comite Institucional para el Cuidado y Uso de los Animales de Laboratorio), and approved by the Ethical Committee of Facultad de Medicina, Universidad Autónoma de Nuevo León (registration number HT17- 00004).

Consent to participate Not applicable.

Consent for publication Not applicable.

Competing interests The authors declare no competing interests.

References

- Anisimov VN, Zabezhinski MA, Popovich IG, Piskunova TS, Semenchenko AV, Tyndyk ML, Yurova MN, Antoch MP, Blagosklonny MV (2010) Rapamycin extends maximal lifespan in cancer-prone mice. *Am J Pathol* 176(5):2092–2097. <https://doi.org/10.2353/ajpath.2010.091050>
- Anisimov VN, Zabezhinski MA, Popovich IG, Piskunova TS, Semenchenko AV, Tyndyk ML, Yurova MN, Rosenfeld SV, Blagosklonny MV (2011) Rapamycin increases lifespan and inhibits spontaneous tumorigenesis in inbred female mice. *Cell Cycle* 10(24):4230–4236. <https://doi.org/10.4161/cc.10.24.18486>
- Arriola Apelo SI, Neuman JC, Baar EL, Syed FA, Cummings NE, Brar HK, Pumper CP, Kimple ME, Lamming DW (2016) Alternative rapamycin treatment regimens mitigate the impact of rapamycin on glucose homeostasis and the immune system. *Aging Cell* 15(1):28–38. <https://doi.org/10.1111/accel.12405>
- Barriocanal-Casado E, Hidalgo-Gutiérrez A, Raimundo N, González-García P, Acuña-Castroviejo D, Escames G, López LC (2019) Rapamycin administration is not a valid therapeutic strategy for every case of mitochondrial disease. *EBioMedicine* 42:511–523. <https://doi.org/10.1016/j.ebiom.2019.03.025>
- Bartolome A, Guillén C (2014) Role of the mammalian target of rapamycin (mTOR) complexes in pancreatic β -cell mass regulation. *Vitam Horm* 95:425–469. <https://doi.org/10.1016/B978-0-12-800174-5.00017-X>
- Blagosklonny MV (2011) Rapamycin-induced glucose intolerance: hunger or starvation diabetes. *Cell Cycle* 10(24):4217–4224. <https://doi.org/10.4161/cc.10.24.18595>
- Blagosklonny MV (2019) Rapamycin for longevity: opinion article. *Aging (Albany NY)* 11(19):8048–8067. <https://doi.org/10.18632/aging.102355>
- Blandino-Rosano M, Barbaresso R, Jimenez-Palomares M, Bozadjieva N, Werneck-de-Castro JP, Hatanaka M, Mirmira RG, Sonenberg N, Liu M, Rüegg MA, Hall MN, Bernal-Mizrachi E (2017) Loss of mTORC1 signalling impairs β -cell homeostasis and insulin processing. *Nat Commun* 8:16014. <https://doi.org/10.1038/ncomm16014>
- Bravo-San Pedro JM, Senovilla L (2013) Immunostimulatory activity of lifespan-extending agents. *Aging (Albany NY)* 5(11):793–801. <https://doi.org/10.18632/aging.100619>
- Campistol JM, Eris J, Oberbauer R, Friend P, Hutchison B, Morales JM, Claesson K, Stallone G, Russ G, Rostaing L, Kreis H, Burke JT, Brault Y, Scarola JA, Neylan JF (2006) Sirolimus therapy after early cyclosporine withdrawal reduces the risk for cancer in adult renal transplantation. *J Am Soc Nephrol* 17(2):581–589. <https://doi.org/10.1681/ASN.2005090993>
- Chong ZZ, Maiese K (2012) Mammalian target of rapamycin signaling in diabetic cardiovascular disease. *Cardiovasc Diabetol* 11:45. <https://doi.org/10.1186/1475-2840-11-45>
- Chong ZZ, Shang YC, Zhang L, Wang S, Maiese K (2010) Mammalian target of rapamycin: hitting the bull's-eye for neurological disorders. *Oxid Med Cell Longev* 3(6):374–391. <https://doi.org/10.4161/oxim.3.6.14787>
- Chong ZZ, Shang YC, Wang S, Maiese K (2012) Shedding new light on neurodegenerative diseases through the mammalian target of rapamycin. *Prog Neurobiol* 99(2):128–148. <https://doi.org/10.1016/j.pneurobio.2012.08.001>
- Civiletto G, Dogan SA, Cerutti R, Fagiolaro G, Moggio M, Lamperti C, Benincá C, Viscomi C, Zeviani M (2018) Rapamycin rescues mitochondrial myopathy via coordinated activation of autophagy and lysosomal biogenesis. *EMBO Mol Med* 10 (11). <https://doi.org/10.15252/emmm.201708799>
- Comas M, Toshkov I, Kuropatwinski KK, Chernova OB, Polinsky A, Blagosklonny MV, Gudkov AV, Antoch MP (2012) New nano-formulation of rapamycin Rapatar extends lifespan in homozygous p53^{-/-} mice by delaying carcinogenesis. *Aging (Albany NY)* 4(10):715–722. <https://doi.org/10.18632/aging.100496>
- Cunningham JT, Rodgers JT, Arlow DH, Vazquez F, Mootha VK, Puigserver P (2007) mTOR controls mitochondrial oxidative function through a YY1-PGC-1 α transcriptional complex. *Nature* 450(7170):736–740. <https://doi.org/10.1038/nature06322>
- Deblon N, Bourgoin L, Veyrat-Durebex C, Peyrou M, Vinciguerra M, Caillon A, Maeder C, Fournier M, Montet X, Rohner-Jeanrenaud F, Foti M (2012) Chronic mTOR inhibition by rapamycin induces muscle insulin resistance despite weight loss in rats. *Br J Pharmacol* 165(7):2325–2340. <https://doi.org/10.1111/j.1476-5381.2011.01716.x>
- Dominguez J, Mahalati K, Kiberd B, McAlister VC, MacDonald AS (2000) Conversion to rapamycin immunosuppression in renal transplant recipients: report of an initial experience. *Transplantation* 70(8):1244–1247. <https://doi.org/10.1097/00007890-200010270-00021>
- Elghazi L, Blandino-Rosano M, Alejandro E, Cras-Méneur C, Bernal-Mizrachi E (2017) Role of nutrients and mTOR signaling in the regulation of pancreatic progenitors development. *Mol Metab* 6(6):560–573. <https://doi.org/10.1016/j.molmet.2017.03.010>
- Felici R, Buonvicino D, Muzzi M, Cavone L, Guasti D, Lapucci A, Pratesi S, De Cesaris F, Luceri F, Chiarugi A (2017) Post onset, oral rapamycin treatment delays development of mitochondrial encephalopathy only at supramaximal doses. *Neuropharmacology* 117:74–84. <https://doi.org/10.1016/j.neuropharm.2017.01.039>
- García-Martínez JM, Alessi DR (2008) mTOR complex 2 (mTORC2) controls hydrophobic motif phosphorylation and activation of serum- and glucocorticoid-induced protein kinase 1 (SGK1). *Biochem J* 416(3):375–385. <https://doi.org/10.1042/BJ20081668>
- Goldberg EL, Smithey MJ, Lutes LK, Uhrlaub JL, Nikolich-Zugich J (2014) Immune memory-boosting dose of rapamycin impairs macrophage vesicle acidification and curtails glycolysis in effector CD8 cells, impairing defense against acute infections. *J Immunol* 193(2):757–763. <https://doi.org/10.4049/jimmunol.1400188>
- Graziotto JJ, Cao K, Collins FS, Krainc D (2012) Rapamycin activates autophagy in Hutchinson-Gilford progeria syndrome: implications for normal aging and age-dependent neurodegenerative disorders. *Autophagy* 8(1):147–151. <https://doi.org/10.4161/auto.8.1.18331>
- Guertin DA, Stevens DM, Thoreen CC, Burds AA, Kalaany NY, Moffat J, Brown M, Fitzgerald KJ, Sabatini DM (2006) Ablation in mice of the mTORC components raptor, rictor, or mLST8 reveals that mTORC2 is required for signaling to Akt-FOXO and PKC α , but not S6K1. *Dev Cell* 11(6):859–871. <https://doi.org/10.1016/j.devcel.2006.10.007>
- Gyurus E, Kaposztas Z, Kahan BD (2011) Sirolimus therapy predisposes to new-onset diabetes mellitus after renal transplantation: a long-term analysis of various treatment regimens. *Transplant Proc* 43(5):1583–1592. <https://doi.org/10.1016/j.transproceed.2011.05.001>
- Heuer M, Dreger NM, Cicinnati VR, Fingas C, Juntermanns B, Paul A, Kaiser GM (2012) Tumor growth effects of rapamycin on human

- biliary tract cancer cells. *Eur J Med Res* 17:20. <https://doi.org/10.1186/2047-783X-17-20>
- Houde VP, Brûlé S, Festuccia WT, Blanchard PG, Bellmann K, Deshaies Y, Marette A (2010) Chronic rapamycin treatment causes glucose intolerance and hyperlipidemia by upregulating hepatic gluconeogenesis and impairing lipid deposition in adipose tissue. *Diabetes* 59(6):1338–1348. <https://doi.org/10.2337/db09-1324>
- Ikenoue T, Inoki K, Yang Q, Zhou X, Guan KL (2008) Essential function of TORC2 in PKC and Akt turn motif phosphorylation, maturation and signalling. *EMBO J* 27(14):1919–1931. <https://doi.org/10.1038/emboj.2008.119>
- Jeon HJ, Lee HE, Yang J (2018) Safety and efficacy of Rapamune® (Sirolimus) in kidney transplant recipients: results of a prospective post-marketing surveillance study in Korea. *BMC Nephrol* 19(1):201. <https://doi.org/10.1186/s12882-018-1002-6>
- Jiang J, Zuo Y, Gu Z (2013) Rapamycin protects the mitochondria against oxidative stress and apoptosis in a rat model of Parkinson's disease. *Int J Mol Med* 31(4):825–832. <https://doi.org/10.3892/ijmm.2013.1280>
- Johnson SC, Rabinovitch PS, Kaerberlein M (2013) mTOR is a key modulator of ageing and age-related disease. *Nature* 493(7432):338–345. <https://doi.org/10.1038/nature11861>
- Johnson SC, Yanos ME, Kayser EB, Quintana A, Sangesland M, Castanza A, Uhde L, Hui J, Wall VZ, Gagnidze A, Oh K, Wasko BM, Ramos FJ, Palmiter RD, Rabinovitch PS, Morgan PG, Sedensky MM, Kaerberlein M (2013) mTOR inhibition alleviates mitochondrial disease in a mouse model of Leigh syndrome. *Science* 342(6165):1524–1528. <https://doi.org/10.1126/science.1244360>
- Johnson SC, Yanos ME, Bitto A, Castanza A, Gagnidze A, Gonzalez B, Gupta K, Hui J, Jarvie C, Johnson BM, Letexier N, McCanta L, Sangesland M, Tamis O, Uhde L, Van Den Ende A, Rabinovitch PS, Suh Y, Kaerberlein M (2015) Dose-dependent effects of mTOR inhibition on weight and mitochondrial disease in mice. *Front Genet* 6:247. <https://doi.org/10.3389/fgene.2015.00247>
- Johnston O, Rose CL, Webster AC, Gill JS (2008) Sirolimus is associated with new-onset diabetes in kidney transplant recipients. *J Am Soc Nephrol* 19(7):1411–1418. <https://doi.org/10.1681/ASN.2007111202>
- Jung CH, Ro SH, Cao J, Otto NM, Kim DH (2010) mTOR regulation of autophagy. *FEBS Lett* 584(7):1287–1295. <https://doi.org/10.1016/j.febslet.2010.01.017>
- Kahan BD, Podbielski J, Napoli KL, Katz SM, Meier-Kriesche HU, Van Buren CT (1998) Immunosuppressive effects and safety of a sirolimus/cyclosporine combination regimen for renal transplantation. *Transplantation* 66(8):1040–1046. <https://doi.org/10.1097/00007890-199810270-00013>
- Kauffman HM, Cherikh WS, Cheng Y, Hanto DW, Kahan BD (2005) Maintenance immunosuppression with target-of-rapamycin inhibitors is associated with a reduced incidence of de novo malignancies. *Transplantation* 80(7):883–889. <https://doi.org/10.1097/01.tp.0000184006.43152.8d>
- Khan NA, Nikkanen J, Yatsuga S, Jackson C, Wang L, Pradhan S, Kivelä R, Pessia A, Velagapudi V, Suomalainen A (2017) mTORC1 regulates mitochondrial integrated stress response and mitochondrial myopathy progression. *Cell Metab* 26(2):419–428. <https://doi.org/10.1016/j.cmet.2017.07.007>
- Khanna AK (2000) Mechanism of the combination immunosuppressive effects of rapamycin with either cyclosporine or tacrolimus. *Transplantation* 70(4):690–694. <https://doi.org/10.1097/00007890-200008270-00027>
- Krebs M, Brunmair B, Brehm A, Artwohl M, Szendroedi J, Nowotny P, Roth E, Fürnsinn C, Promintzer M, Anderwald C, Bischof M, Roden M (2007) The Mammalian target of rapamycin pathway regulates nutrient-sensitive glucose uptake in man. *Diabetes* 56(6):1600–1607. <https://doi.org/10.2337/db06-1016>
- Lamming DW, Ye L, Katajisto P, Goncalves MD, Saitoh M, Stevens DM, Davis JG, Salmon AB, Richardson A, Ahima RS, Guertin DA, Sabatini DM, Baur JA (2012) Rapamycin-induced insulin resistance is mediated by mTORC2 loss and uncoupled from longevity. *Science* 335(6076):1638–1643. <https://doi.org/10.1126/science.1215135>
- Lamming DW, Ye L, Sabatini DM, Baur JA (2013) Rapalogs and mTOR inhibitors as anti-aging therapeutics. *J Clin Invest* 123(3):980–989. <https://doi.org/10.1172/JCI64099>
- Lamming DW (2016) Inhibition of the mechanistic target of rapamycin (mTOR)-rapamycin and beyond. *Cold Spring Harb Perspect Med* 6(5). <https://doi.org/10.1101/cshperspect.a025924>
- Lebranchu Y (2010) Can we eliminate both calcineurin inhibitors and steroids? *Transplant Proc* 42(9 Suppl):S25–28. <https://doi.org/10.1016/j.transproceed.2010.07.002>
- Lebwohl D, Anak O, Sahmoud T, Klimovsky J, Elmroth I, Haas T, Posluszny J, Saletan S, Berg W (2013) Development of everolimus, a novel oral mTOR inhibitor, across a spectrum of diseases. *Ann N Y Acad Sci* 1291:14–32. <https://doi.org/10.1111/nyas.12122>
- Leontieva OV, Demidenko ZN, Blagosklonny MV (2014) Rapamycin reverses insulin resistance (IR) in high-glucose medium without causing IR in normoglycemic medium. *Cell Death Dis* 5:e1214. <https://doi.org/10.1038/cddis.2014.178>
- Li S (2009) The possible cellular mechanism for extending lifespan of mice with rapamycin. *Biol Proced Online* 11:1–2. <https://doi.org/10.1007/s12575-009-9015-y>
- Li W, Zhang H, Nie A, Ni Q, Li F, Ning G, Li X, Gu Y, Wang Q (2016) mTORC1 pathway mediates beta cell compensatory proliferation in 60 % partial-pancreatectomy mice. *Endocrine* 53(1):117–128. <https://doi.org/10.1007/s12020-016-0861-5>
- Liu P, Wang Z, Wei W (2014) Phosphorylation of Akt at the C-terminal tail triggers Akt activation. *Cell Cycle* 13(14):2162–2164. <https://doi.org/10.4161/cc.29584>
- Long SA, Rieck M, Sanda S, Bollyky JB, Samuels PL, Goland R, Ahmann A, Rabinovitch A, Aggarwal S, Phippard D, Turka LA, Ehlers MR, Bianchine PJ, Boyle KD, Adah SA, Bluestone JA, Buckner JH, Greenbaum CJ, Network DTatIT (2012) Rapamycin/IL-2 combination therapy in patients with type 1 diabetes augments Tregs yet transiently impairs β -cell function. *Diabetes* 61(9):2340–2348. <https://doi.org/10.2337/db12-0049>
- Longo VD, Fontana L (2011) Intermittent supplementation with rapamycin as a dietary restriction mimetic. *Aging (Albany NY)* 3(11):1039–1040. <https://doi.org/10.18632/aging.100401>
- Malagelada C, Jin ZH, Jackson-Lewis V, Przedborski S, Greene LA (2010) Rapamycin protects against neuron death in in vitro and in vivo models of Parkinson's disease. *J Neurosci* 30(3):1166–1175. <https://doi.org/10.1523/JNEUROSCI.3944-09.2010>
- Mannick JB, Del Giudice G, Lattanzi M, Valiante NM, Praestgaard J, Huang B, Lonetto MA, Maecker HT, Kovarik J, Carson S, Glass DJ, Klickstein LB (2014) mTOR inhibition improves immune function in the elderly. *Sci Transl Med* 6(268):268ra179. <https://doi.org/10.1126/scitranslmed.3009892>
- Mannick JB, Morris M, Hockey HP, Roma G, Beibel M, Kulmatycki K, Watkins M, Shavlakadze T, Zhou W, Quinn D, Glass DJ, Klickstein LB (2018) TORC1 inhibition enhances immune function and reduces infections in the elderly. *Sci Transl Med* 10(449). <https://doi.org/10.1126/scitranslmed.aag1564>
- Mathew T, Kreis H, Friend P (2004) Two-year incidence of malignancy in sirolimus-treated renal transplant recipients: results from five multicenter studies. *Clin Transplant* 18(4):446–449. <https://doi.org/10.1111/j.1399-0012.2004.00188.x>
- McCormack FX, Inoue Y, Moss J, Singer LG, Strange C, Nakata K, Barker AF, Chapman JT, Brantly ML, Stocks JM, Brown KK, Lynch JP, Goldberg HJ, Young LR, Kinder BW, Downey GP, Sullivan EJ, Colby TV, McKay RT, Cohen MM, Korbbe L,

- Taveira-DaSilva AM, Lee HS, Krischer JP, Trapnell BC, Consortium NIOHRLD, Group MT (2011) Efficacy and safety of sirolimus in lymphangi leiomyomatosis. *N Engl J Med* 364(17):1595–1606. <https://doi.org/10.1056/NEJMoa1100391>
- Mendelsohn AR, Larrick JW (2011) Rapamycin as an antiaging therapeutic?: targeting mammalian target of rapamycin to treat Hutchinson-Gilford progeria and neurodegenerative diseases. *Rejuvenation Res* 14(4):437–441. <https://doi.org/10.1089/rej.2011.1238>
- Mohacsi PJ, Morris RE (1992) Brief treatment with rapamycin in vivo increases responsiveness to alloantigens measured by the mixed lymphocyte response. *Immunol Lett* 34(3):273–278. [https://doi.org/10.1016/0165-2478\(92\)90224-c](https://doi.org/10.1016/0165-2478(92)90224-c)
- Nair AB, Jacob S (2016) A simple practice guide for dose conversion between animals and human. *J Basic Clin Pharm* 7(2):27–31. <https://doi.org/10.4103/0976-0105.177703>
- Noda T, Ohsumi Y (1998) Tor, a phosphatidylinositol kinase homologue, controls autophagy in yeast. *J Biol Chem* 273(7):3963–3966. <https://doi.org/10.1074/jbc.273.7.3963>
- Poüs C, Codogno P (2011) Lysosome positioning coordinates mTORC1 activity and autophagy. *Nat Cell Biol* 13(4):342–344. <https://doi.org/10.1038/ncb0411-342>
- Ramirez-Moreno MJ, Duarte-Jurado AP, Gopar-Cuevas Y, Gonzalez-Alcocer A, Loera-Arias MJ, Saucedo-Cardenas O, Montes de Oca-Luna R, Rodriguez-Rocha H, Garcia-Garcia A (2019) Autophagy stimulation decreases dopaminergic neuronal death mediated by oxidative stress. *Mol Neurobiol*. <https://doi.org/10.1007/s12035-019-01654-1>
- Rosado C, García-Cosmes P, Fraile P, Vázquez-Sánchez F (2013) Tuberous sclerosis associated with polycystic kidney disease: effects of rapamycin after renal transplantation. *Case Rep Transplant* 2013:397087. <https://doi.org/10.1155/2013/397087>
- Ru W, Peng Y, Zhong L, Tang SJ (2012) A role of the mammalian target of rapamycin (mTOR) in glutamate-induced down-regulation of tuberous sclerosis complex proteins 2 (TSC2). *J Mol Neurosci* 47(2):340–345. <https://doi.org/10.1007/s12031-012-9753-1>
- Sarbassov DD, Ali SM, Sengupta S, Sheen JH, Hsu PP, Bagley AF, Markhard AL, Sabatini DM (2006) Prolonged rapamycin treatment inhibits mTORC2 assembly and Akt/PKB. *Mol Cell* 22(2):159–168. <https://doi.org/10.1016/j.molcel.2006.03.029>
- Sarkar S, Krishna G, Imarisio S, Saiki S, O’Kane CJ, Rubinsztein DC (2008) A rational mechanism for combination treatment of Huntington’s disease using lithium and rapamycin. *Hum Mol Genet* 17(2):170–178. <https://doi.org/10.1093/hmg/ddm294>
- Saunders RN, Metcalfe MS, Nicholson ML (2001) Rapamycin in transplantation: a review of the evidence. *Kidney Int* 59(1):3–16. <https://doi.org/10.1046/j.1523-1755.2001.00460.x>
- Schreiber KH, Ortiz D, Academia EC, Anies AC, Liao CY, Kennedy BK (2015) Rapamycin-mediated mTORC2 inhibition is determined by the relative expression of FK506-binding proteins. *Aging Cell* 14(2):265–273. <https://doi.org/10.1111/accel.12313>
- Schriever SC, Deutsch MJ, Adamski J, Roscher AA, Ensenauer R (2013) Cellular signaling of amino acids towards mTORC1 activation in impaired human leucine catabolism. *J Nutr Biochem* 24(5):824–831. <https://doi.org/10.1016/j.jnutbio.2012.04.018>
- Selman C, Partridge L (2012) A double whammy for aging? Rapamycin extends lifespan and inhibits cancer in inbred female mice. *Cell Cycle* 11(1):17–18. <https://doi.org/10.4161/cc.11.1.18736>
- Siegmund SE, Yang H, Sharma R, Javors M, Skinner O, Mootha V, Hirano M, Schon EA (2017) Low-dose rapamycin extends lifespan in a mouse model of mtDNA depletion syndrome. *Hum Mol Genet* 26(23):4588–4605. <https://doi.org/10.1093/hmg/ddx341>
- Sinagoga KL, Stone WJ, Schiesser JV, Schweitzer JI, Sampson L, Zheng Y, Wells JM (2017) Distinct roles for the mTOR pathway in postnatal morphogenesis, maturation and function of pancreatic islets. *Development* 144(13):2402–2414. <https://doi.org/10.1242/dev.146316>
- Teutonico A, Schena PF, Di Paolo S (2005) Glucose metabolism in renal transplant recipients: effect of calcineurin inhibitor withdrawal and conversion to sirolimus. *J Am Soc Nephrol* 16(10):3128–3135. <https://doi.org/10.1681/ASN.2005050487>
- Tremblay F, Krebs M, Dombrowski L, Brehm A, Bernroider E, Roth E, Nowotny P, Waldhäusl W, Marett A, Roden M (2005) Overactivation of S6 kinase 1 as a cause of human insulin resistance during increased amino acid availability. *Diabetes* 54(9):2674–2684. <https://doi.org/10.2337/diabetes.54.9.2674>
- Tsang CK, Qi H, Liu LF, Zheng XF (2007) Targeting mammalian target of rapamycin (mTOR) for health and diseases. *Drug Discov Today* 12(3–4):112–124. <https://doi.org/10.1016/j.drudis.2006.12.008>
- Vander Haar E, Lee SI, Bandhakavi S, Griffin TJ, Kim DH (2007) Insulin signalling to mTOR mediated by the Akt/PKB substrate PRAS40. *Nat Cell Biol* 9(3):316–323. <https://doi.org/10.1038/ncb1547>
- Volunteers AH (2002) Guidance for industry and reviewers. Center for Biologics Evaluation and Research (CBER)
- Wang Y, Liu Y, Lu J, Zhang P, Xu Y, Wang Z, Mao JH, Wei G (2013) Rapamycin inhibits FBXW7 loss-induced epithelial-mesenchymal transition and cancer stem cell-like characteristics in colorectal cancer cells. *Biochem Biophys Res Commun* 434(2):352–356. <https://doi.org/10.1016/j.bbrc.2013.03.077>
- Wataya-Kaneda M, Tanaka M, Nakamura A, Matsumoto S, Katayama I (2012) A novel application of topical rapamycin formulation, an inhibitor of mTOR, for patients with hypomelanotic macules in tuberous sclerosis complex. *Arch Dermatol* 148(1):138–139. <https://doi.org/10.1001/archderm.148.1.138>
- Wicker LS, Boltz RC, Matt V, Nichols EA, Peterson LB, Sigal NH (1990) Suppression of B cell activation by cyclosporin A, FK506 and rapamycin. *Eur J Immunol* 20(10):2277–2283. <https://doi.org/10.1002/eji.1830201017>
- Xie J, Herbert TP (2012) The role of mammalian target of rapamycin (mTOR) in the regulation of pancreatic β -cell mass: implications in the development of type-2 diabetes. *Cell Mol Life Sci* 69(8):1289–1304. <https://doi.org/10.1007/s00018-011-0874-4>

Publisher's note Springer Nature remains neutral with regard to jurisdictional claims in published maps and institutional affiliations.